Appl. Phys. A 69 [Suppl.], S49–S53 (1999) / Digital Object Identifier (DOI) 10.1007/s003399900340

Applied Physics A
Materials
Science & Processing

Theory for laser-induced ultrafast phase transitions in carbon

H.O. Jeschke, M.E. Garcia, K.H. Bennemann

Institut für Theoretische Physik der Freien Universität Berlin, Arnimallee 14, 14195 Berlin, Germany

Received: 21 July 1999/Accepted: 15 September 1999/Published online: 28 December 1999

Abstract. The response of carbon to femtosecond laser pulses of arbitrary form, different durations, and different intensities is studied theoretically. We perform molecular dynamics simulations based on a microscopic electronic Hamiltonian. We include in our model the theoretical description of the pulse form, the electron thermalization, and diffusion effects explicitly. We apply our method to diamond and C_{60} crystals. For the diamond case, we show that a femtosecond laser pulse induces a nonequilibrium transition to graphite, which takes place for a wide range of pulse durations and intensities. This ultrafast collective motion of the atoms occurs within a time scale shorter than 100 fs. The laser-induced melting of a C_{60} crystal under pressure is also analyzed. In this case, an ultrafast melting of the system occurs. We discuss the mechanisms underlying these nonequilibrium phase transitions.

PACS: 81.05.Tp; 79.20.Ds; 61.80.Az

As a consequence of the interaction between intense femtosecond laser pulses and a semiconductor or insulator, a dense electron-hole plasma is excited, which induces dramatic changes in the interactions between the atoms. Thus, during this short-lived nonequilibrium situation, bond-breaking and bond-formation processes occur that usually result in very fast nonthermal phase transitions.

In recent years a lot of experimental evidence for the existence of laser-induced ultrafast phase transitions has been obtained [1–10]. In many experiments on different materials, a variety of laser-induced ultrafast phenomena has been observed, as for instance femtosecond melting [1–4, 6–8], subpicosecond disorder–order transitions [9, 10], and nonthermal ablation [1–4, 6–10].

In most of these investigations either the initial or the final state was a noncrystalline one (liquid or amorphous solid). However, a laser-induced transition between two crystalline structures is also possible, namely the graphitization of diamond. It has been experimentally shown that laser pulses induce a graphitization of a diamond surface [5].

The thermal transition from diamond to graphite is an old problem, and the mechanism of graphitization upon heating is already known. When the system is heated in such a way that the atoms acquire enough kinetic energy to overcome the potential barrier between diamond and graphite, the graphitization takes place. Recently, a theoretical study of the graphitization of an (111)-diamond film under heating was reported by Car and coworkers [11], who performed molecular dynamics simulations at constant temperature. Taking into account that the response of solids to ultrashort laser pulses is characterized by nonequilibrium processes, one expects a nonequilibrium graphitization of diamond to also occur. Regarding this transition, many questions arise; for instance, is the graphitization mechanism the same as in the thermal case? What are the time scales for the structural transformation? In this paper, we address these problems and perform calculations to clarify this point.

In recent years different experimental groups have undertaken various attempts to achieve the transition from graphite or graphite-like systems to diamond. Different techniques have been used, ranging from irradiation with highly energetic electrons [12] to laser heating of HOPG [13] or of graphitic samples under pressure [14]. Other graphite-like systems could also be a good starting point for the synthesis of diamond or diamond-like carbon. Examples of such compounds are C_{60} molecular crystals, which consist of C_{60} molecules arranged in close-packed fcc structures [15]. We present in this paper calculations of the response of a C_{60} crystal to a femtosecond laser pulse. We show that under certain conditions (external pressure, high intensities and short pulse durations), the system melts and could condense into diamond-like carbon.

Recently, different theoretical methods have been developed and used to simulate laser-induced ultrafast phase transitions [16–19]. In all theoretical works, a nonthermal melting of different materials was obtained. This is not surprising, since the mentioned simulations have been performed

COLA'99 – 5th International Conference on Laser Ablation, July 19–23, 1999 in Göttingen, Germany

at constant volume (density). Note that under this constraint, the solid is not allowed to expand, and the excess excitation energy is only redistributed among the atomic degrees of freedom. Consequently, the system either melts or, if the excess energy is not large enough, remains in the original lattice structure.

In this paper we analyze the laser-induced graphitization of diamond by allowing volume changes, since, for instance, crystalline diamond and graphite have rather different densities. Our study concentrates on a subregion in the center of the irradiated area that can change its structure, form, and volume rapidly. In this way, and in contrast to the case of constant volume, part of the energy pumped into the system by the laser pulse is spent for expansion or deformation, preventing ultrafast melting [20]. Furthermore, the system is allowed to explore new lattice structures, which are unavailable if the volume is kept constant.

The paper is organized as follows. In Sect. 1 we outline our theoretical approach. In Sect. 2 we present the results of our molecular dynamics simulations. Finally, in Sect. 3 we summarize our results.

1 Theory

Our physical picture for the interaction of the ultrashort laser pulse and diamond is the following. Because of the action of the pulse, electrons are excited from occupied to unoccupied levels with a time-dependent probability which is proportional to the intensity of the laser field. As a consequence of this extremely fast excitation process, a nonequilibrium distribution of electrons is created. Through electron–electron collisions, this distribution converges (within a characteristic time scale) to an equilibrium (Fermi-like) occupation of the electronic levels. In parallel to this thermalization process, diffusion from the excited region into the rest of the material sets in. During this complex electron dynamics, the atoms do not remain fixed at their equilibrium positions but undergo a relaxation process triggered by the dramatic changes in the potential energy surface (PES). This structural relaxation may terminate in another crystal phase of the system.

From the above discussion, it is clear that a description of laser-induced nonequilibrium structural phase transitions requires one to take into account as many atomic degrees of freedom as possible. As was mentioned before, we analyze the dynamics of the system at constant pressure. For this purpose, we employ a molecular dynamics (MD) technique proposed by Parrinello and Rahman [21] that is based upon a Lagrangian of the form

$$L(t) = \sum_{i=1}^{N} \frac{m_i}{2}\, \dot{\boldsymbol{s}}_i^T\, h^T\, h\, \dot{\boldsymbol{s}}_i - \sum_{\substack{i=1\\ j\neq i}}^{N} \Phi(r_{ij}, t) + K - P\Omega\,. \tag{1}$$

Here, the coordinates $\boldsymbol{s}_i$ of the N atoms are taken relative to the vectors $\boldsymbol{a}$, $\boldsymbol{b}$, and $\boldsymbol{c}$ that form the MD supercell. These primitive vectors form the columns of the matrix $h = (\boldsymbol{a}\,\boldsymbol{b}\,\boldsymbol{c})$. The absolute coordinates of the atoms are given by $\boldsymbol{r}_i = h\boldsymbol{s}_i$. W is a parameter with the dimension of mass, $\Omega = \det(h)$ is the volume of the MD supercell, and P is the external pressure. The second term represents the PES, which is determined from a microscopic theory as described below. The first two terms of the Lagrangian would lead to the usual Newton equations of motion, while the third and fourth terms are introduced to simulate the time evolution of the MD unit cell, the coordinates of which are considered as 9 extra degrees of freedom. The third term, K, describes the kinetic energy of the MD supercell. In the original theory of Parrinello and Rahman [21], the third term is written as $K_{\mathrm{PR}} = 1/2W\mathrm{Tr}(\dot{h}^T\dot{h})$, whereas the improved version due to Cleveland [22], which is independent of the choice of the MD supercell, reads $K_{\mathrm{C}} = 1/2W\mathrm{Tr}(\dot{h}\sigma^T\sigma\dot{h}^T)$ with $\sigma_{\alpha\beta} = \partial\Omega/\partial h_{\alpha\beta}$. We used both approaches and obtained identical results. It has been shown that the Lagrangian L leads to the correct isoenthalpic, isobaric ensemble averages up to order $1/N$ [26].

Through the use of the Euler–Lagrange formalism, $N+9$ equations of motion for the atomic coordinates $\boldsymbol{s}_i$ and for the MD cell coordinates h_{kl} are derived from (1) by the use of K_{PR} for the third term:

$$\ddot{\boldsymbol{s}}_i = -\frac{1}{m_i}\sum_{j\neq i}\frac{\partial\Phi(r_{ij})}{\partial r_{ij}}\frac{(\boldsymbol{s}_i - \boldsymbol{s}_j)}{r_{ij}} - g^{-1}\dot{g}\dot{\boldsymbol{s}}_i \tag{2}$$

$$\ddot{h} = \frac{1}{W\Omega}\left(\sum_{i=1}^{N} m_i \boldsymbol{v}_i\boldsymbol{v}_i^T - \sum_{i=1}^{N}\sum_{j>i}\frac{\partial\Phi(r_{ij})}{\partial r_{ij}}\frac{\boldsymbol{r}_{ij}\boldsymbol{r}_{ij}^T}{r_{ij}} - P\right)\sigma \tag{3}$$

where $g = h^T h$, $\boldsymbol{v}_i = h\dot{\boldsymbol{s}}_i$ and $\sigma_{\alpha\beta} = \frac{\partial\Omega}{\partial h_{\alpha\beta}}$.

The forces which enter the equations of motion as $\mathrm{d}\Phi(r_{ij})/\mathrm{d}\boldsymbol{s}_k$ are determined by the use of the Born–Oppenheimer approximation and are given by

$$\boldsymbol{f}_i = -\sum_m n(\varepsilon_m, t)\,\langle m|\frac{\partial H}{\partial \boldsymbol{s}_i}|m\rangle - \frac{\partial E_{\mathrm{rep}}}{\partial \boldsymbol{s}_i}, \tag{4}$$

in which m labels the electronic levels, which are the eigenstates of the electronic Hamiltonian $H(\boldsymbol{r}_1, \ldots, \boldsymbol{r}_N)$. $E_{\mathrm{rep}}(\boldsymbol{r}_1, \ldots, \boldsymbol{r}_N)$ contains the repulsive interactions between the atomic cores. For the derivation of (4), the Hellmann–Feynman theorem has been used. The forces for the MD supercell $f_{\alpha\beta}^h$ are calculated analogously:

$$f_{\alpha\beta}^h = -\sum_m n(\varepsilon_m, t)\,\langle m|\frac{\partial H}{\partial h_{\alpha\beta}}|m\rangle - \frac{\partial E_{\mathrm{rep}}}{\partial h_{\alpha\beta}}. \tag{5}$$

In (4), $n(\varepsilon_m, t)$ refers to the occupation of the energy level ε_m at time t. This time-dependent occupation changes because of the action of the laser pulse, Coulomb interactions, and diffusion effects. The occupation $n(\varepsilon_m, t)$ is initially given by a Fermi distribution at the temperature of the lattice. During the excitation by the laser pulse, this distribution changes in time according to

$$\begin{aligned}\frac{\mathrm{d}n(\varepsilon_m, t)}{\mathrm{d}t} = &\int_{-\infty}^{\infty}\mathrm{d}\omega\, g(\omega, t-\tau)\Big\{[n(\varepsilon_m - \hbar\omega, t-\tau)\\ &+ n(\varepsilon_m + \hbar\omega, t-\tau) - 2n(\varepsilon_m, t-\tau)]\Big\}\\ &- \frac{n(\varepsilon_m, t) - n^0(\varepsilon_m)}{\tau_1}.\end{aligned} \tag{6}$$

Here, the first term describes the laser-induced excitation processes $\varepsilon_m \to \varepsilon_m \pm \hbar\omega$, which are weighted by the spectral function $g(\omega, t)$ of the laser pulse at each time step τ. The second term of (6) takes into account, in a simple approximation, the thermalization processes due to electron–electron collisions. The nonequilibrium distribution $n_{\varepsilon_m}(t)$ relaxes towards a Fermi distribution $n^0(\varepsilon_m) = 2/\{\exp[(\varepsilon_m - \mu)/k_B T_e(t)] + 1\}$ with an (energy-independent) time constant τ_1.

The time-dependent electron temperature $T_e(t)$ contained in $n^0_{\varepsilon_m}$ is obtained from the time evolution of the total energy

$$E_t(t) = \sum_{\substack{i=1 \\ j\neq i}}^{N} \Phi(r_{ij}, t) + E_{\mathrm{kin}}(t) = E_t(t=0) + E_{\mathrm{abs}}(t)\,, \qquad (7)$$

where $E_{\mathrm{kin}}(t)$ is the kinetic energy of the atoms and $E_{\mathrm{abs}}(t)$ is the energy that has already been absorbed from the laser pulse at time t. The PES is determined by $\sum_{i=1}^{N}\sum_{j\neq i}\Phi(r_{ij}, t) = \sum_m n(\varepsilon_m, t)\varepsilon_m(\boldsymbol{r}_1, \ldots, \boldsymbol{r}_N)$, where ε_m are the eigenvalues of the Hamiltonian

$$H = \sum_{i\alpha} \epsilon_{i\alpha} n_{i\alpha} + \sum_{\substack{ij\alpha\beta \\ j\neq i}} V_{ij}^{\alpha\beta}(r_{ij}) c_{i\alpha}^{+} c_{j\beta}. \qquad (8)$$

Here, $\epsilon_{i\alpha}$ is the on-site energy of atom i and orbital α. $c_{i\alpha}^{+}$ and $c_{j\alpha}$ are the creation and annihilation operators, and $V_{ij}^{\alpha\beta}(r_{ij})$ the hopping integrals. For the description of carbon, the $2s$, $2p_x$, $2p_y$, and $2p_z$ orbitals are taken into account. For the radial part of the hopping integrals and for E_{rep}, we employ the forms proposed by Xu, et al. [25]:

$$S(r) = \begin{cases} \left(\frac{r_0}{r}\right)^n \exp\left\{n\left[-\left(\frac{r}{r_c}\right)^{n_c} + \left(\frac{r_0}{r_c}\right)^{n_c}\right]\right\}, & r < r_1 \\ d_0 + d_1(r-r_1) + d_2(r-r_1)^2 + d_3(r-r_1)^3, & r \geq r_1 \end{cases} \qquad (9)$$

$$E_{\mathrm{rep}} = \sum_i f\Big(\sum_j \phi(r_{ij})\Big) \qquad \text{with} \qquad (10)$$

$$\phi(r) = \begin{cases} \phi_0\left(\frac{d_0}{r}\right)^m \exp\left\{m\left[-\left(\frac{r}{d_c}\right)^{m_c} + \left(\frac{d_0}{d_c}\right)^{m_c}\right]\right\}, & r < d_1 \\ c_0 + c_1(r-d_1) + c_2(r-d_1)^2 + c_3(r-d_1)^3, & r \geq d_1. \end{cases} \qquad (11)$$

Thus, for distances $r > r_1$ and $r > d_1$ respectively, the hopping integrals and $\phi(r)$ are replaced by polynomials that go to zero and are fitted smoothly to the functions valid for $r < r_1$ and $r < d_1$. The repulsive potential E_{rep} is taken as a polynomial of the function $\phi(r)$. For all parameters in (9)–(11), see [25].

At the short time scale of a few picoseconds, the main process causing dissipation of the absorbed energy is the diffusion of hot electrons into the surrounding cold lattice. This is taken into account by a further rate equation

$$\frac{\mathrm{d}T_e(t)}{\mathrm{d}t} = -\frac{T_e(t) - T_l(t)}{\tau_2}; \qquad (12)$$

i.e., within a diffusion time constant τ_2, the electron temperature $T_e(t)$ approaches the lattice temperature $T_l(t)$.

2 Results

In this section we present results for the response of a diamond and a C_{60} molecular crystal to a femtosecond laser pulse. We model the laser pulse by a Gaussian envelope of duration τ. The parameter W was adjusted so that the fluctuations of the MD cell volume Ω, in the electronic ground state of the system, take place on a time scale of $\sqrt[3]{\Omega}/c_{\mathrm{M}}$, where c_{M} is the speed of sound in the material.

In the diamond case, we consider a molecular dynamics supercell consisting of 216 atoms and periodic boundary conditions. The external pressure is 1 atm.

In Fig. 1 we show, for given values of τ and E_{abs}, an example of the ultrafast graphitization in the (110)-direction of the diamond crystal. The 216-atom sample of diamond was excited by a 20 fs laser pulse, and the four panels in Fig. 1 show snapshots of the structure at different times: the bent hexagons of the diamond lattice in the (110) direction break up to form the even planes of graphite, while in the direction perpendicular to the newly formed planes, the originally bent hexagons become flat and form the even hexagons of the graphite lattice. Note that in this newly formed graphite lattice, which is in a high vibrational excitation, the planes are still all equivalent, and the familiar structure of hexagonal and rhombohedral graphite with layering sequences of ABABAB and ABCABC, respectively, has not yet been formed. Although it is to be expected that the graphite formed here will eventually relax towards one of these two standard structures of graph-

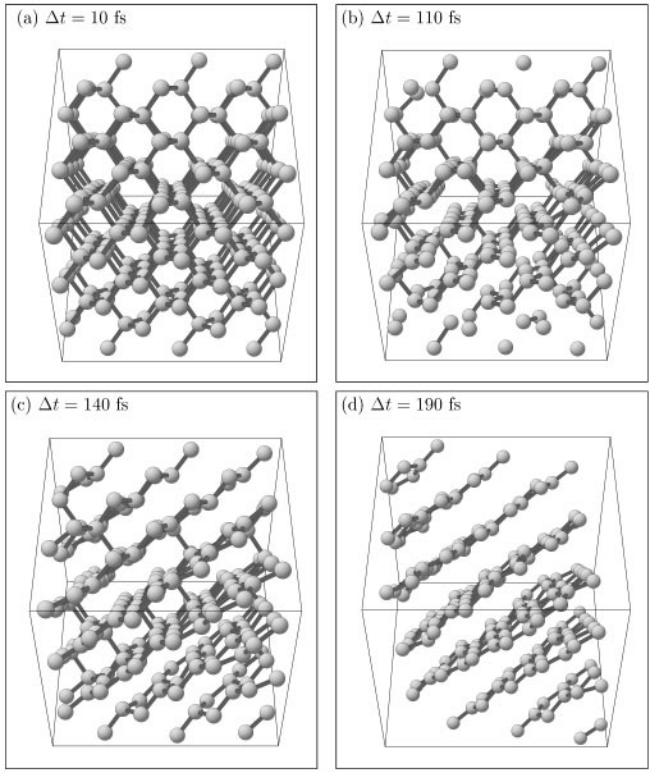

Fig. 1. Snapshots in the (110) direction of the ultrafast dynamics of diamond ($N = 216$ atoms) upon excitation with a laser pulse of duration $\tau = 20$ fs (Gaussian shape). Δt is the time delay with respect to the peak of the pulse. The energy absorbed is $E_{\mathrm{abs}} = 1.1$ eV/atom. The graphitization of diamond takes less than 100 fs. Bonds longer than 1.6 Å are not shown

ite, in the tight binding method, no energy difference between different layer arrangements is observed because the interplane van der Waals interactions are not taken into account.

For the simulation of the ultrafast relaxation of a C_{60} molecular crystal, we consider a supercell of 240 atoms and periodic boundary conditions. The external pressure is 10 GPa.

In Fig. 2 we show snapshots of the destruction of a C_{60} molecular crystal induced by intense laser irradiation. The laser pulse is characterized by a duration of $\tau = 20$ fs, and during its action an energy of $E_{\mathrm{abs}} = 3.6$ eV/atom is absorbed by the lattice. A constant external isotropic pressure of $P = 10$ GPa is applied to the system at all times. In the figure, we indicate bonds up to a length of 1.6 Å with dark grey, while bonds between 1.6 Å and 2.1 Å in length are shaded in light grey and have a smaller diameter. Bonds longer than 2.1 Å are not shown, as they contribute only negligibly to the binding energy, and thus atoms that are more than 2.1 Å apart can be considered unbound. At $\Delta t = 0$ fs (Fig. 2a), i.e., at the pulse maximum, the atoms have not yet had time to react to the change in the PES due to the absorption of nearly half of the laser intensity; they still form the perfect fcc lattice of the solid C_{60} at 300 K. The fact that in each of the C_{60} molecules a few atoms seem to be missing, while several atoms can be seen that are not directly connected to one of the four C_{60} molecules, is a consequence of the periodic boundary conditions. The six atoms on the bottom left of the first panel, for example, actually form a part of the C_{60} molecule in the background. At $\Delta t = 20$ fs (Fig. 2b), the C_{60} molecules have expanded considerably, as can be seen from the many light grey (i.e., stretched) bonds that have replaced dark grey ones. At $\Delta t = 60$ fs (Fig. 2c), the expansion of the C_{60} molecules has proceeded beyond the elastic limit of the C–C bonds, and the original form of the C_{60} molecules appears mainly in the large hollow spaces not yet filled in by the hot carbon atoms. Through the collision processes between the fragments of the C_{60} molecules, the kinetic energy of the system has now increased by 2200 K to $T_l = 2500$ K. At $\Delta t = 160$ fs (Fig. 2d), the fragments of the destroyed C_{60} molecules have filled up most of the available space, and the distribution of matter approaches homogeneity. Up to a time delay of approximately $\Delta t = 120$ fs, the volume of the system has decreased very rapidly by 30% because the resistance of the nearly incompressible C_{60} molecules to the external pressure has vanished. The panels for $\Delta t = 260$ fs and $\Delta t = 860$ fs (Fig. 2e,f) show rapid structural rearrangements of the very hot ($T_l \approx 3000$–3500 K) material. The density at $\Delta t = 860$ fs is $\varrho = 2.5$ g/cm^3. A very long simulation of several hundred picoseconds will be needed to determine the final structure of the material after cooling takes place through slow processes like heat diffusion.

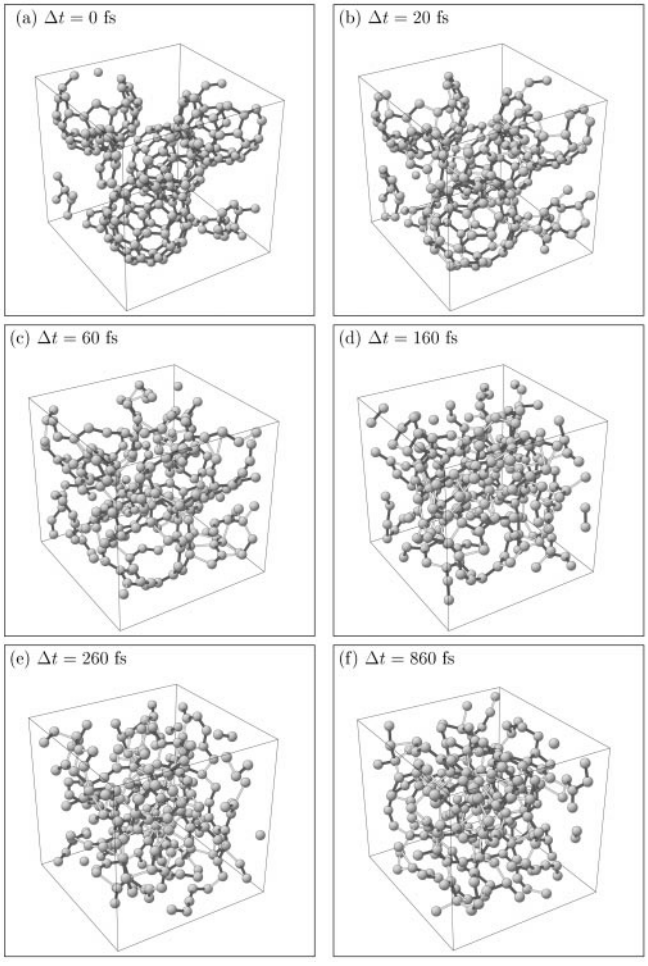

Fig. 2. Snapshots of a C_{60} molecular crystal during and after irradiation by an ultrashort laser pulse. Pulse duration is $\tau = 20$ fs; an energy of $E_{\mathrm{abs}} = 3.6$ eV/atom is absorbed during the laser excitation. A constant external pressure of $p = 10$ GPa acts on the crystal. Time delays Δt are given with respect to the peak of the pulse. Bonds up to a length of 1.6 Å are shown in dark grey, and bonds between 1.6 Å and 2.1 Å in length are shown in light grey and are thinner in diameter. For a detailed discussion of the dynamics, please refer to the text

In Fig. 3 we show the densities of state of (a) diamond in the ground state and (b) the same system after excitation with a laser pulse of $\tau = 20$ fs duration that leads to an ultrafast graphitization of the sample. The trajectory is the same as that from which the snapshots displayed in Fig. 1 are taken. During the laser pulse, an energy of $E_{\mathrm{abs}} = 1.1$ eV/atom is absorbed by the system. The Fermi level ε_{F} is indicated by a vertical line. The structure in the DOS close to the Fermi level in Fig. 3 reflects the high vibrational excitation of the graphite planes; in the course of the graphiti-

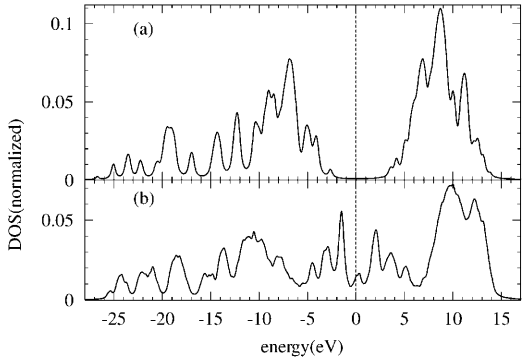

Fig. 3. Densities of state of diamond (a) before and (b) after irradiation by a laser pulse of $\tau = 20$ fs duration. In the course of the excitation, an energy of $E_{\mathrm{abs}} = 1.1$ eV/atom is absorbed. The DOS (b) is calculated at a time $t = 190$ fs after the pulse maximum. This figure corresponds to the graphitization trajectory shown in Fig. 1; (a) is the DOS for the structure in Fig. 1a, and (b) is that for Fig. 1d. The energy $\varepsilon = 0$ refers to the Fermi level ε_{F}, which is also indicated by a *vertical line*

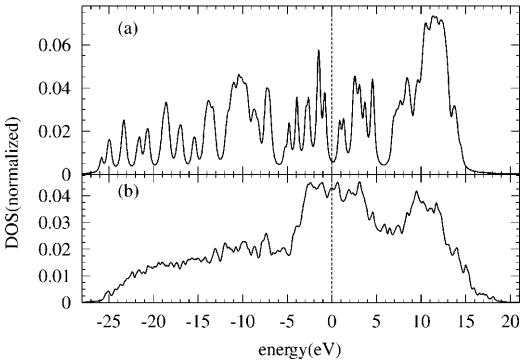

Fig. 4. Densities of state of a C_{60} molecular crystal (a) before and (b) after irradiation by a laser pulse of $\tau = 20$ fs duration. In the course of the excitation, an energy of $E_{\text{abs}} = 3.6$ eV/atom is absorbed. The DOS (b) is calculated at a time $t = 860$ fs after the pulse maximum. This figure corresponds to the trajectory shown in Fig. 2; (a) is the DOS for the structure in Fig. 2a, (b) is that for Fig. 2f. The energy $\varepsilon = 0$ refers to the Fermi level ε_{F}, which is also indicated by a *vertical line*

zation process the lattice temperature has risen by 1300 K to a value of $T_l = 1600$ K. This temperature increase results from the difference in potential energy between the electronically excited diamond structure, that at the time of the graphitization is not a minimum of the PES any more, and the lower lying graphite minimum of the PES. Thus, the DOS in Fig. 3b will approach the equilibrium DOS of graphite only after several hundreds or even thousands of picoseconds, when the heat in the lattice has had time to decrease to its previous value through processes like heat conduction.

In Fig. 4 the densities of state of the C_{60} molecular crystal before and after laser irradiation are presented. The laser pulse has a duration of $\tau = 20$ fs, and the system absorbs an energy of $E_{\text{abs}} = 3.6$ eV/atom. The DOS in Fig. 4b corresponds to the last panel of Fig. 2 and is thus taken at a time delay of $\Delta t = 860$ fs after the pulse maximum. It is clear that the small energy gap of solid C_{60} at the Fermi level that can be seen in Fig. 4a has been filled with states in the course of the collapse of the C_{60} molecules, and the DOS in Fig. 4b is metallic-like.

3 Summary

We have calculated the response of diamond and a C_{60} crystal to ultrafast laser pulses. We have obtained a femtosecond crystalline solid to crystalline solid transition consisting in a graphitization of diamond. This transition occurs for a wide range of pulse durations and intensities. This study opens up the possibility of control of the end product of the laser excitation (e.g., graphite or liquid carbon). Our results are independent of the functional form for the kinetic energy of the MD supercell, and also of the size of the MD supercell, at least for $N = 64$ and $N = 216$. For the ultrafast dynamics of a C_{60} molecular crystal under pressure, we obtain a rapid melting of the system shortly after the laser excitation. Although we cannot make predictions about the final state after cooling, formation of sp^3 bonds might be favored, since the density of the intermediate liquid state decreases with increasing time.

Acknowledgements. This work has been supported by the Deutsche Forschungsgemeinschaft through SFB 450. Our simulations were done on the CRAY T3E at Konrad-Zuse-Zentrum für Informationstechnik Berlin.

References

1. H.W.K. Tom, G.D. Aumiller, C.H. Brito-Cruz: Phys. Rev. Lett. **60**, 1438 (1988)
2. K. Sokolowski-Tinten, J. Bialkowski, D. von der Linde: Phys. Rev. B **51**, 14 186 (1995) and references therein
3. D.H. Reize, H. Ahn, M.C. Downer: Phys. Rev. B **45**, 2677 (1992)
4. T. Dallas, M. Holtz, H. Ahn, M.C. Downer: Phys. Rev. B **49**, 796 (1994)
5. S. Preuss, M. Stuke: Appl. Phys. Lett. **67**, 338 (1995)
6. I.L. Shumay, U. Höfer: Phys. Rev. B **53**, 15 878 (1996)
7. P. Saeta, J.-K. Wang, Y. Siegal, N. Bloembergen, E. Mazur: Phys. Rev. Lett. **67**, 1023 (1991)
8. L. Huang, J.P. Callan, E.N. Glezer, E. Mazur: Phys. Rev. Lett. **80**, 185 (1998)
9. J. Solis, C.N. Afonso, S.C.W. Hyde, N.P. Barry, P.M.W. French: Phys. Rev. Lett. **76**, 2519 (1996)
10. K. Sokolowski-Tinten, J. Solis, J. Bialkowski, J. Siegel, C.N. Afonso, D. von der Linde (unpublished)
11. A. De Vita, G. Galli, A. Canning, R. Car: Nature (London) **379**, 523 (1996)
12. Y. Lyutovich, F. Banhart: Appl. Phys. Lett. **74**, 659 (1999)
13. A. Mechler, P. Heszler, Z. Kántor, T. Szörényi, Z. Bor: Appl. Phys. A **66**, 659 (1998)
14. H. Yusa, K. Takemura, Y. Matsui, H. Morishima, K. Watanabe, H. Yamawaki, K. Aoki: Appl. Phys. Lett. **72**, 1843 (1998)
15. S. Saito, A. Oshiyama: Phys. Rev. Lett. **66**, 2637 (1991)
16. P. Stampfli, K.H. Bennemann: Phys. Rev. B **42**, 7163 (1990); Phys. Rev. B **49**, 7299 (1994)
17. P.L. Silvestrelli, A. Alavi, M. Parrinello, D. Frenkel: Phys. Rev. Lett. **77**, 3149 (1996)
18. P.L. Silvestrelli, M. Parrinello: J. Appl. Phys. **83**, 2478 (1998)
19. S. Das Sarma, J.R. Senna: Phys. Rev. B **49**, 2443 (1994)
20. H.O. Jeschke, M.E. Garcia, K.H. Bennemann: Phys. Rev. B **60**, R3701 (1999)
21. M. Parrinello, A. Rahman: J. Appl. Phys. **52**, 7182 (1981)
22. C.L. Cleveland: J. Chem. Phys. **89**, 4987 (1988)
23. H.C. Andersen: J. Chem. Phys. **72**, 2384 (1980)
24. F.P. Bundy, W.A. Bassett, R.S. Weathers, R.J. Hemley, H.K. Mao, A.F. Goncharov: Carbon **34**, 141 (1996)
25. For more details, see C.H. Xu, C.Z. Wang, C.T. Chan, K.M. Ho: J. Phys.: Condens. Matter **4**, 6047 (1992)
26. H.C. Andersen: J. Chem. Phys. **72**, 2384 (1980)